13th Australasian Fluid Mechanics Conference
Monash University, Melbourne, Australia
13-18 December 1998

APPLICATION OF PHASE CONTRAST MAGNETIC RESONANCE IMAGING TO FLOW MEASUREMENT

Brett R. COWAN[1], Gordon D. MALLINSON[2], Sai Kit CHEUNG[2] and Sung Kit MAN[2]

[1]Department of Medicine
[2]Department of Mechanical Engineering
The University of Auckland, Auckland, NEW ZEALAND

ABSTRACT

A medical magnetic resonance imaging (MRI) system has been used to measure flow in benchmark fluid mechanics problems to assess the accuracy and utility of the technology for measuring fluid motion. This paper concentrates on the first of these studies, flow in a pipe for Reynolds numbers up to 5000. The accuracy and detail of the results demonstrate the enormous potential that MRI has for fluid mechanics research.

INTRODUCTION

The intensity of an MRI image obtained using a phase encoded sequence is modulated by the fluid velocity in the direction of phase encoding. For a given imaging plane, three phase encoded images can be used to construct a map of the three dimensional velocity field in that plane. By sweeping through a volume using a sequence of imaging planes, a complete representation of a three dimensional flow can be obtained. A medical MRI system can produce phase encoded images for a 256 by 256 grid of 1 mm pixels in a few seconds which means that a complete measurement of a steady or repetitive flow can be completed in a few minutes.

A medical MRI system is most sensitive to the motion of water or other fluids having a similar density of hydrogen atoms. It is non-invasive. There is no requirement for seeding the fluid and the walls do not need to be transparent. As far as application to engineering flows is concerned, the flow apparatus must be sufficiently small to be inserted inside the magnet and large enough that 1mm pixels will resolve the flow. The apparatus must not contain ferrous or other magnetic materials nor, ideally, any conductor in which induced eddy currents may reduce system accuracy or produce unwanted heating effects.

The capabilities of MRI for flow measurement have been recognised previously with laboratory MRI systems being used to investigate a range of fluid mechanics problems (Callahan 1995). Phantoms used in Medical MRI systems have demonstrated the viability of the technique for flow measurement (Ku *et al* 1990). Recently the value of MRI flow measurement to validate CFD results has been indicated (Newling *et al* 1997) but the situations were sufficiently complex that the accuracy of the CFD modelling could be questioned.

In this investigation situations have been chosen to progress from unidirectional flow to three-dimensional flow with a view to establishing detailed benchmark comparisons.

METHODS

Three separate experiments (phantoms) have been constructed to create one, two and three dimensional flows.

Straight Pipe

Water was pumped at flow rates up to 100 ml/sec (Re_D<5000) through a 21.2 mm internal diameter circular cross section straight plastic pipe. The pipe passed through a head coil, (designed to image the human head), that was used by the system to apply the excitation pulses and detect echoes that were then processed to produce the images. The mass flow and water density were independently measured with a Micro Motion Coriolis flow meter to an accuracy of 0.2%. The pipe was sufficiently long to ensure that the flow was fully developed at the measurement cross section.

Sudden Expansion

The pipe apparatus was modified so that its diameter increased abruptly from 21.2 to 37.1 mm. The same range of flows could be studied and the flow rate was measured with the same equipment.

Rotating Flow

A vertical cylindrical container 40 mm in diameter and 70 mm high was filled with water. Either the cylinder or its lid could be rotated by a purpose built water motor constructed entirely from non metallic materials. The lid or the body of the chamber could be driven to generate different kinds of rotating flows.

Results for only the first two of these examples are presented in this paper.

Imaging and Processing

Standard phase encoding sequences were used on a Siemens 1.5 Tesla magnet. A single image acquisition can use a number of measurements which are averaged. The sensitivity of a sequence is defined by its velocity encoding (VENC) value. Averages from 1 to 10 and VENC values from 2 to 500 cm/sec were used.

The images were assembled to form velocity vector fields by using purpose written software. Processing and visualisation tasks used an adapted version of the *SeeFD* CFD visualisation software at the University of Auckland.

STRAIGHT PIPE

Volume flow rate

This study was done to determine the accuracy with which steady flow could be measured and is the one for which the most analysis has been completed. The results presented here were obtained from single direction phase encoded images that were sensitive to flow along the pipe.

Images were obtained for 12 flow rates and a set were taken for stationary water to provide zero offsets. Several VENC settings and averages were used for each flow rate so that a total of 217 images were obtained. Each measurement produced a standard intensity image as well as the phase encoded image.

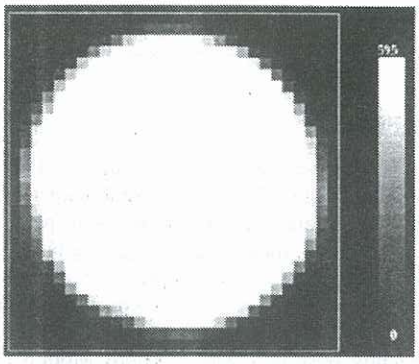

Figure 1: Intensity image of the cross section of a 21.2 i.d. pipe containing water, Re = 800.

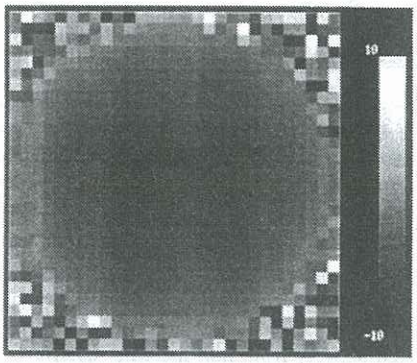

Figure 2: Phase encode image of the flow in Figure 1. The VENC is 10.

The field of view setting meant that the pipe intersected approximately 600 pixels that were 0.781 mm square. The intensity image (Figure 1) clearly shows the interior of the pipe where the bright pixels represent water. The dimmer pixels near the pipe wall contain both water and the wall material. Pixels completely in the wall or the external air are black. As will be discussed later, one of the issues associated with data processing is that of correctly determining the position of the wall.

Figure 2 shows a phase encoded image in which the intensity of pixels completely filled with water is proportional to the velocity through the image plane. Those not containing water have a nearly random intensity as seen in the corner regions of Figure 2.

In order to estimate the flow rate from the MRI measurements the following steps were taken.

- Pixels having intensity values greater than a prescribed threshold were included in a filter used to process the phase encoded images. The threshold was chosen so that the number of pixels accepted corresponded to the known cross sectional area of the pipe.
- A flow rate for each phase encoded image was calculated using algebraic summation of the products of the pixel velocity values and their areas.
- These data were used to produce over all correlations of flow rate against the measurements made by the Coriolis meter.

The regressions having the best fit were those where the zero flow offset was taken into account and when 3 or 10 averages were taken. The results from various values of VENC showed that as expected, the optimum VENC was the lowest that could accommodate the maximum velocity in the flow.

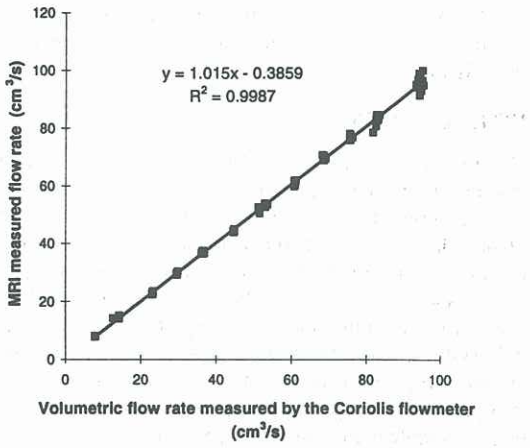

Figure 3: Regression line for MRI measurement of flow rate against independent measurements by a Coriolis flow meter.

The regression line in Figure 3 is for all data. For images based on 10 averages and VENC of 40, a correlation over 7 flow rates had a slope of 1.0076 an offset of -0.0356. For 3 averages and 12 flow rates, the slope was 1.0153, and the intercept -0.4664. In both cases the correlation coefficient (R^2) was better than 0.999.

Velocity profiles

Figure 4 shows the velocity profiles in the pipe. Because the profiles have been scaled by the volume flow rate, their height is an inverse indication of the "flatness" of the profile. The surfaces in Figure 4 have been generated by drawing triangles between the raw numerical data. Note that the lowest flow is showing evidence of noise, but this decreases as Re approaches the lower limit of transition. At Re = 2430, the profile has started to depart from the laminar parabolic profile and may also be not fully developed. By Re = 5000, the much flatter turbulent profile is clearly evident.

(While the overall flow rates are clearly being measured accurately, it should be remembered when examining the velocity profiles that the data for an MRI image are acquired by scanning the frequency domain. The image

from which the velocities are computed is an inverse Fourier transformation of those data.)

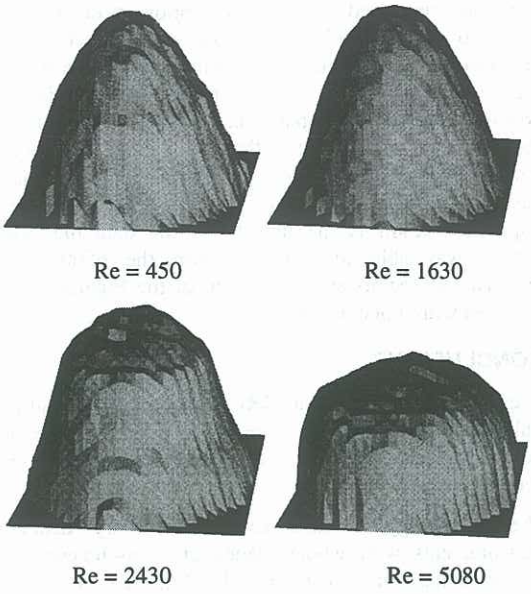

Figure 4: Velocity profile surfaces in the pipe as measured by MRI. The profiles have been scaled by the volume flow rate.

The accuracy of measurement of local velocity was assessed by fitting a parabolic velocity profile to the velocity data. The function,

$$w = a_1x^2 + a_2xy + a_3y^2 + a_4x + a_5y + a_6 \quad (1)$$

was fitted using least squares and used to estimate the centre of the velocity profile which was then written as

$$w_{max} - w = \frac{(x-x_c)^2}{a^2} + \frac{(y-y_c)^2}{b^2} \quad (2)$$

From this equation the diameter of the pipe and the volume flow rate were estimated by,

$$d = 2\sqrt{\pi a b w_{max}} \qquad V = \tfrac{1}{2}\pi a b w_{max}{}^2 \quad (3)$$

By expressing the locations of the pixels in terms of their radii from the centre, a cylindrical profile

$$w_{max} - w = \frac{r^2}{c^2} \quad (4)$$

could be refitted to the data. From (4)

$$d' = 2c\sqrt{\pi w_{max}} \qquad V' = \tfrac{1}{2}\pi c^2 w_{max}{}^2 \quad (5)$$

The results process so far have indicated that the two estimates of diameter and flow rate agree to 4 significant figures.

Examples of the results of this process are in Figures 5 and 6. Figure 5(a) shows the 'cloud' of data points obtained from the phase encoded image. The fitted profile in (b) is clearly close. In Figure 6 the cylindrical parabola has been drawn as a net that represents the location of the pipe as detected by processing the flow data. It is seen to be in good agreement with the intensity image. The comparison in the Figure is typical of that obtained with all sets of laminar flow data. There is a slight shift of the net relative to the intensity image and the diameter of the pipe is over predicted by between 2 and 3 per cent. The flow is well centred but for this Reynolds number the contours of velocity near the peak are slightly elliptic.

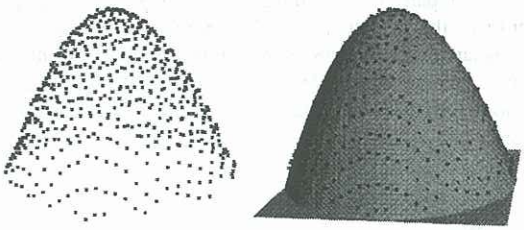

Figure 5: Measured data (a) and a fitted cylindrical profile (b) for Re = 800.

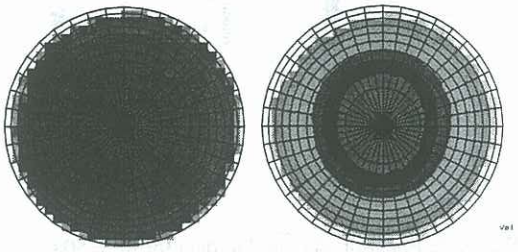

Figure 6: Fitted parabolic net superimposed on the (a) intensity and (b) flow contour maps for Re = 800.

Re	Flow rate	Flow - MRI 1	Flow MRI 2	d (full)	d (part)
	cm^3/s	/Measured		/2.18 mm	
452	7.95	0.993	0.991	1.032	1.032
800	14.29	0.981	0.978	1.033	1.033
1290	23.28	0.988	0.986	1.015	1.012
1630	29.60	1.002	1.004	1.018	1.017
1990	36.50	1.008	1.012	1.018	1.018
2430	44.55	0.993	1.003	1.044	1.039
2910	53.63	0.997	1.009	1.047	1.030
3300	61.10	1.007	1.040	1.093	1.042
3690	68.50	1.011	1.284	1.237	1.054
4090	76.12	0.999	1.19	1.285	1.068
5080	94.73	1.010	1.25	1.331	1.076

Table 1: Comparison of flow rates estimated by (MRI 1) algebraic summation and (MRI 2) integration of a fitted quadratic profile. Estimated diameters are based on quadratic profiles fitted to (full) all the data or (part) velocities less than half the peak.

The fitted parabolic profile can be used to estimate the volume flow rate. The data in Table 1 provide a comparison between this method (MRI 2) and that of simply summing the contributions of the individual pixels (MRI 1). Clearly it is inappropriate to use the parabolic profile to estimate the flow rate for turbulent flow as evidenced by the increasing errors beyond Re = 2430.

Similarly, while the parabolic profile provides a good estimate of the pipe diameter for laminar flow, it rapidly becomes inadequate for turbulent flow. This error can be significantly reduced by fitting the parabola to the lower half of the velocity profile as illustrated in Figure 8. The estimated diameter from all the data is 28.19 mm. For the lower half of the profile it is 22.8 mm.

The estimation of the position of vessel walls is an important part of MRI image processing. These results confirm the viability of the process suggested by Ringgaard *et al* (1998) and Penderson *et al* (1998) in which parabolic profiles are fitted to the boundary regions of blood vessel flow to determine the size of the vessel.

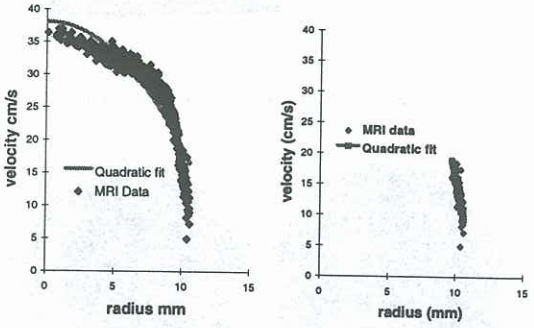

(a) (b)

Figure 8: Equation (4) fitted to data for Re = 5080. In(a) all data have been used, In (b) velocities less than half the peak have been used.

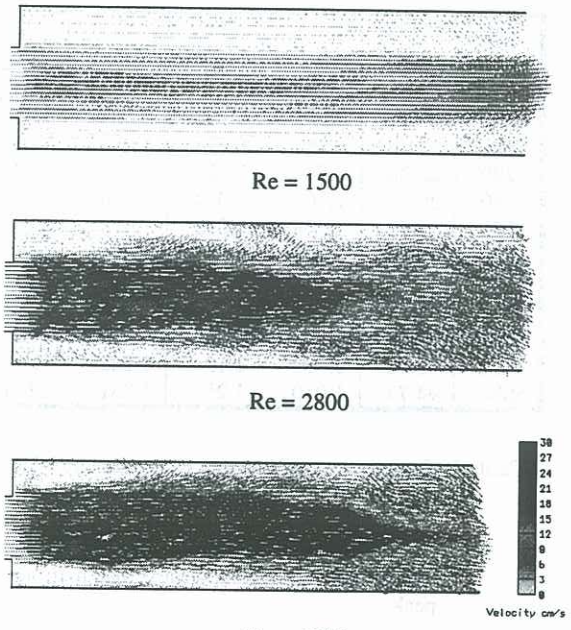

Figure 9: Flow vectors for 3 values of Re (based on the lesser diameter) through a step expansion. All maps use the same vector scale factor and grey scale.

Sudden Expansion

The results presented here are based on measurements in a single vertical plane. Three directions of phase encoding were used to yield the motion in the vertical plane so that the velocity vectors are, in fact, three-dimensional. Typical results are shown in Figure 9. For the laminar flow the point of reattachment is far downstream from the expansion. For the turbulent flow, the point of re-attachment of the flow is approximately 3 diameters downstream from the expansion. These data have yet to be completely analysed but already the most impressive result is the density of the data the MRI system was able to produce, with the 6500 three dimensional vectors shown in each of the Figures being acquired within one minute.

CONCLUSIONS

These results indicate that MRI is capable of measuring fluid motion to a high degree of accuracy. For steady flow with no acceleration, fluid velocity can be measured better than 1.5%.

The technology is also capable of very detailed measurements with whole planes of three-dimensional vectors being acquired in seconds. A most encouraging indication is the potential that the technique has for the verification of CFD predictions of three dimensional steady fluid motion.

ACKNOWLEDGEMENTS

The support of the University of Auckland Research Committee and Manukau Radiology Institute Limited is gratefully acknowledged.

REFERENCES

CALLAGHAN, P.T., NMR Imaging in Rheology, *Proc. 12th Australasian Fluid Mechanics Conference*, Sydney 195-200. 1995.

KU, D.N., BIANCHERI, C.L., PETTIGREW, R.I., PEIFER, J.W., MARKOU, C.P., ENGELS, H., Evaluation of Magnetic Resonance Velocimetry for Steady Flow, *Journal of Biomechanical Engineering*, 112, 464-472 1990.

NEWLING, B. GIBBS, S.J., DERBYSHIRE, J.A., XING, D., HALL, L.D., HAYCOCK, D.E., FRITH, W.J., ABLET, S., Comparisons of Magnetic Resonance Imaging Velocimetry with Computational Fluid Dynamics, *Journal of Fluids Engineering*, 119, 103-109, 1997.

PENDERSON, E.S., AGERBAEK, M., KRISTENSEN, I.B., SCHEIDEGGER, M., KORZERKE, S., BOESIGER, S., OYRE, S., Abdominal aortic wall shear stress measured by multiple sectored three-dimensional paraboloid fitting of MR velocity data. Correlation with histopathology, *Proc ISMRM*, 6, 476, 1998.

RINGGAARD, S., OYRE, S., PAASKE, W.P., KOZERKE,S., BOESIGER, P., PENDERSEN, E.M., Accurate Automatic Determination of Blood Flow, Vessel Area and Wall Shear Stress by Modelling of Magnetic Resonance Velocity Data from the Common Carotid Artery, *Proc ISMRM*, 6, 2149, 1998.